LONG WAVELENGTH ASTROPHYSICS

by

Liam Dean Connor

A thesis submitted in conformity with the requirements
for the degree of Doctor of Philosophy
Graduate Department of Astronomy and Astrophysics
University of Toronto

# Abstract

Long wavelength astrophysics

Liam Dean Connor

Doctor of Philosophy

Graduate Department of Astronomy and Astrophysics

University of Toronto

2016

# Acknowledgements

# Contents

# List of Tables

# Chapter 1

# Fast Radio Burst Statistics

This chapter was adapted from three separate papers published in the Monthly Notices of the Royal Astronomical Society that explored the statistics of FRBs. In (Connor et al., 2016c), or "FRB repetition and non-Poissonian statistics", it was argued that FRBs may repeat with unusual statistics. Connor et al. (2016a), or "Constraints on the FRB rate at 700-900 MHz", provided detailed constraints on the FRB rate below L-band, and in "The Euclidean distribution of Fast Radio Bursts" we discussed the best way of calculating $N(> S)$ (Oppermann et al., 2016).

## 1.1 Chapter Overview

In this chapter we discuss a number of statistical issues related to FRBs. Although the Lorimer burst was discovered in 2007, in 2013 there were still fewer than half a dozen detected events. That meant inference about the nature of FRBs based on their statistics was difficult, and early statistical claims seemed to us to over-reach. For example, Petroff et al. (2014) claimed that the absence of events in the lower-latitude components of the High Time Resolution Universe Survey (HTRU) compared to the higher-latitude region was significant at the level of 99.5%, based on four FRBs the high-lat region. Furthermore, this dearth at low latitudes was reportedly significant enough to require something beyond heightened scattering and effective system temperature in the Galactic plane. This prompted explanations for why there might be so many more off the plane than near it (Macquart & Johnston, 2015). However, we found the discrepancy to be less severe by a factor of a few, and that even with five more events in the high-lat component of HTRU there is still less than a $2\sigma$ disagreement. This work is discussed in Sect. 1.5, as adapted from (Connor et al., 2016d).

We have also attempted to urge the community not to jump the gun on the nature

and location of FRBs. Before FRB 121102, by far the most popular class of explanations for FRBs was the cosmological cataclysmic one. This is the scenario in which the IGM accounts for nearly all of the burst's DM, and the pulse is caused by a one-off event, like merging compact objects. Keane et al. (2016a), for example, interpreted diminishing radio emission from a galaxy at $z \approx 0.5$ (giving the DM they would expect), as an FRB host galaxy and afterglow from coalescing neutron stars. This claimed was later questions by Williams & Berger (2016), who suggested this was AGN variability, and not a transient. Before the discovery of FRB 121102's repeat bursts, we suggested that the limits on repetition might be weakened if they repeated with non-Poissonian statistics, and that the repeating scenario ought not be ruled out (Connor et al., 2016f,d). We discuss this work in Sect. 1.3.

Another statistical approach to probing the location of fast radio bursts is to use their flux distribution $N(> S)$. We find in Sect. 1.6 that given the detected events at the time of this writing, the distribution of FRBs is consistent with a Euclidean one. A recent paper (Vedantham et al., 2016) has attempted to model the Parkes beam in order to infer information about the true brightness of bursts it has seen, and we will discuss this briefly in the conclusions.

Finally, calculating and discussing the event rate of FRBs requires some statistical care. In Sect. 1.4 we make the first estimate of the burst rate below 1.4 GHz. We also discuss the problems related to quoting an all-sky rate above a strict fluence threshold, and instead offer a more direct method of predicting a rate for a given telescope. This work was first published in (Connor et al., 2016a).

## 1.2 Introduction

## 1.3 Rethinking the constraints on repetition

Though no source has been shown with certainty to repeat, the limits on repeatability of FRBs are still weak. Several models generically predict repetition, whether periodic or stochastic. Galactic flaring stars (Maoz et al., 2015), radio-bursting magnetars (Popov & Postnov, 2007; Pen & Connor, 2015), and pulsar planet systems (Mottez & Zarka, 2014) all predict repetition with varying rates and burst distributions.

In Connor et al. (2015) it was suggested that supergiant pulses from very young pulsars in supernova remnants of nearby galaxies could explain the high DMs, Faraday rotation, scintillation, and polarization properties of the observed FRBs. We proposed that if the repetition of supergiant pulses were non-Poissonian (with a pink or red distribution) then

one might expect several bursts in a short period of time. It is also worth mentioning that the statistics and repeat rates of FRBs could vary from source to source – even if they come from a single class of progenitors – so a long follow-up on an individual burst may not provide global constraints. In this chapter we will refer to stationary Poisson processes (expectation value, $\mu(t)$, is constant in time) as "Poissonian". When we discuss non-Poissonian statistics we will be focusing on stochastic processes that are correlated on varying timescales. For example we will not discuss periodic signals, which are not Poissonian but have already been studied (Petroff et al., 2015c).

### 1.3.1   Flicker noise

Pink noise is ubiquitous in physical systems, showing up in geology and meteorology, a number of astrophysical sources including quasars and the sun, human biology, nearly all electronic devices, finance, and even music and speech (Press, 1978; Voss & Clarke, 1975). Though there is no agreed-upon mathematical explanation for this phenomenon (Milotti, 2002), fluctuations are empirically known to be inversely proportional to frequency for a variety of dynamical systems. This can be written as

$$S(f) = \frac{C}{f^\gamma} \quad \text{if} \quad f_{\min} \leq f \leq f_{\max}, \tag{1.1}$$

where $S(f)$ is the spectral density (i.e. power spectrum), $\gamma$ is typically between 0.5-2, and $f_{\min}$ and $f_{\max}$ are frequency cutoffs beyond which the power law does not hold. In this chapter we will describe these distributions as having flicker noise.

In the case of a time-domain astronomical source, this results in uniformity on short timescales, i.e. a burst of clustered events followed by extended periods of quiescence. If FRBs were to exhibit such flicker noise then their repetition would not only be non-periodic, but would also have a time-varying pulse rate and, more importantly, variance. Therefore the number of events seen in a follow-up observation would depend strongly on the time passed since the initial event.

In Petroff et al. (2015c) the fields of eight FRBs discovered between 2009 and 2013 were followed up from April to October of 2014, for an average of 11.4 hours per field. During this follow-up programme FRB 140514 was found in the same beam as FRB 110220, however the authors argue that it is likely a new source due to its lower DM. After its discovery, the field of 140514 was monitored five more times, starting 41 days later on 2014-06-24, without seeing anything. Under the assumption that 140514 was a new FRB that only showed up in the same field coincidentally and that the repeat rate is constant, Petroff et al. (2015c) rule out repetition with a period $P \leq 8.6$ hours and

reject $8.6 < P < 21$ hours with 90% confidence. However it is possible that one or both of those premises is invalid, so it is useful to explore the possibility of non-stationary repeat rate statistics and repeating FRBs with variable DM.

If the statistics of the FRB's repeat rate were non-Poissonian and initial bursts from FRBs were to have aftershocks similar to earthquakes, then the non-immediate follow-up observations impose far weaker repeat rate limits than has been suggested. We constructed a mock follow-up observation of the eight FRBs whose fields were observed in Petroff et al. (2015c). We then asked how many bursts are seen to repeat if we do an immediate follow-up vs. a follow-up several years after the initial event at times corresponding to the actual observations carried out.

We run a simple Monte Carlo simulation with one sample per hour and a probability of 0.5 that a given sample has a burst in it. The repeat rate of once per two hours is chosen arbitrarily and should not affect the comparison. To get the $1/f^\gamma$ distribution we take an uncorrelated Gaussian time stream centred on 0 and move to Fourier space, then multiply by $f^{\gamma/2}$, which gives a power spectrum with the desired shape. We then inverse Fourier transform back to get the pink or red time stream. We then take samples with a positive value to contain a pulse and samples with a negative value to contain none.. In the stationary Poisson case, the rate of bursts in the immediate follow-up is the same as the multi-year follow-up since all times are statistically equivalent. However with flicker noise the variance is strongly time-dependent. If we imagine an object that repeated on average once per two hours, then if those pulses were Poisson-distributed the probability of seeing zero bursts in 11.4 hours or longer is $\sim 0.007$. With pink noise one expects this roughly 20% of the time, since the system prefers either to be in "on" or "off" mode. If the average repeat period were more like 5-20 hours, then we would often see nothing in a multi-day follow-up observation that took place weeks or years after the initial event.

This is consistent with what Petroff et al. (2015c) saw, though the conclusions differ depending on the assumed statistics. In Fig. 1.1 we show a sample from this simulation for three repeat distributions. The right panel shows how, if an FRB's burst rate has long-term correlations $(1/f^\gamma)$, the likelihood of a repeat is greatly increased if the follow-up observation is immediately after the initial event, rather than months or years after.

## 1.3.2 FRBs 110220 and 140514

Using the event rate of roughly $10^4$ sky$^{-1}$ day$^{-1}$ from Thornton et al. (2013a), it was originally reported that the probability of seeing a new FRB in the field of 110220 during the 85 hours of follow-up was 0.32 (Petroff et al., 2015a). It was then pointed out by
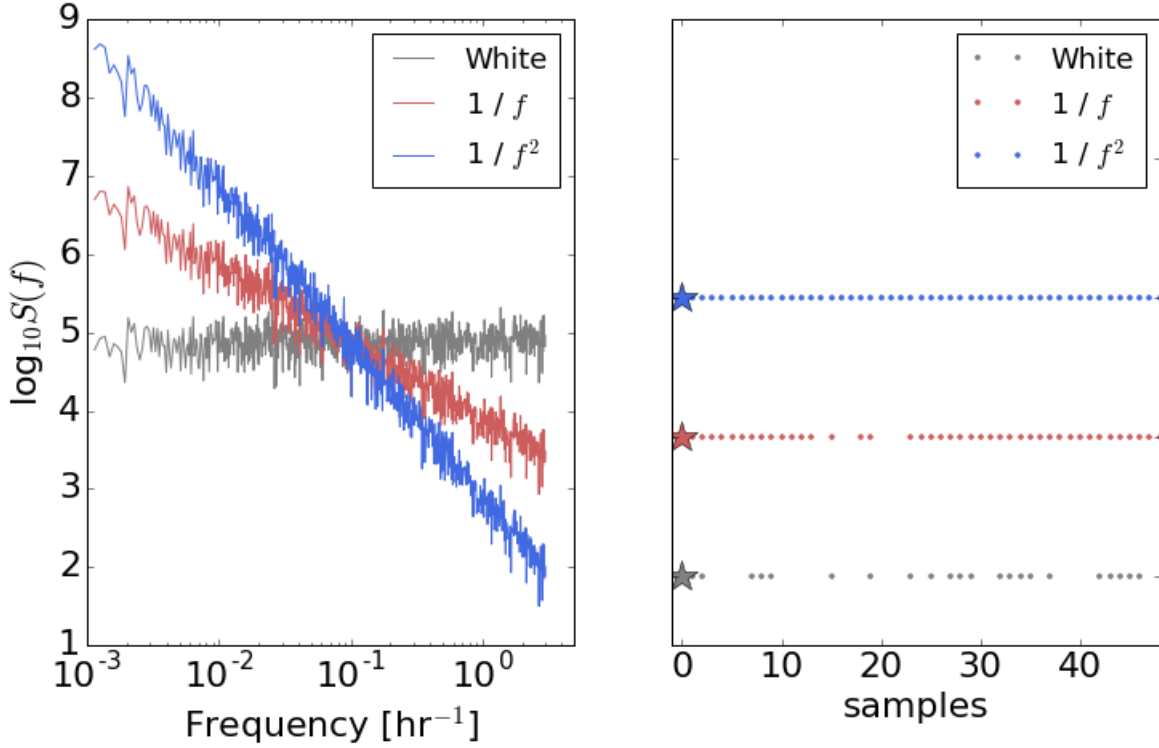
Figure 1.1: Realization of our mock follow-up Monte Carlo. *Left panel*: Power spectrum for pulse arrival times of a single FRB. Grey shows a flat spectrum, corresponding to the often assumed Poissonian repetition rate. The red and blue spectra show flicker noise, with pink $(1/f)$ noise and Brownian $(1/f^2)$ noise respectively. *Right panel*: We found the first "event" in our Monte Carlo (represented by a star) for the three different spectra and plotted their behaviour in the subsequent 48 hours of follow-up. Though the average probability over the whole simulation is 0.5 for each distribution, when we zoom in on this short period the strong time-like correlations in the $1/f^\gamma$ cases means there are many repetitions: they are in an "on" state at this time.

Maoz et al. (2015) that this underestimated the coincidence by an order of magnitude, since they estimated the rate in any one of the 13 beams, while the new event occurred in the identical beam. The probability also dropped due to the updated daily event rate, given the Thornton et al. (2013a) estimate is now thought likely to be too high. In general we expect the true rate of FRBs to be lower than what is reported due to non-publication bias: If archival data are searched and nothing is found, it is less likely to be published than if something is found. That said, using the rate calculated by Rane et al. (2015) and following the procedure of Maoz et al. (2015), we find the likelihood of finding a new burst to be between 0.25-2.5%.

Given the relatively low probability of finding a new FRB in the same field and

since there are models that predict burst repetition with variable DMs (Connor et al., 2015; Maoz et al., 2015) one can ask the question: If one FRB out of eight is found to repeat during 110 hours of follow-up (including extra time spent on 140514), what are the limits on the average repeat period? Another way of asking this question is what is the probability of some number of repetitions during the 110 hours, given a repeat rate. The answer to this question depends strongly on the power spectrum's shape. For the sake of example, if the average repeat rate is once per two hours, then the probability of one repeat or fewer in the Poisson case is effectively zero. With a pink distribution it is closer to 5%, even though the expected number would be 55. This is shown in Fig. 1.2, in which we plot the probability of seeing zero or one repeat burst (the two options for FRB 140514), given some average repetition period, $P$. We generate the pink distribution in the same way described in Section 1.3.1, using one-hour samples and a long-wavelength cutoff at 1.2 million hours. Though it was taken arbitrarily, the probability of seeing no bursts should depend only weakly on this cutoff. Since the variance scales logarithmically with this number, there is only roughly a factor of three difference in total power between our choice and $f_{min} \sim$ an inverse Hubble time. While we remain agnostic about the relationship between 140514 and 110220, with non-Poissonian repetition it is possible to have a relatively high repeat rate and to see either one or zero repeat bursts in several days of observation.

### 1.3.3 Repetition and total number of sources

If FRBs were found to repeat, their statistics and the average frequency of their repetition should affect the search strategy of upcoming surveys. For instance, if it were found that FRBs repeated, on average, five times a day, then the number of unique sources would be five times smaller than the per-sky daily event rate. This means the daily rate $3.3^{+5.0}_{-2.5} \times 10^3$ sky$^{-1}$ estimated by Rane et al. (2015) would be produced by only $\sim$160-1600 sources. In this scenario there is no FRB in most pixels on the sky, which means one could integrate on most patches forever without seeing an event. An example of this strategy is the VLA millisecond search, in which $\sim 40\%$ of the time was spent at a single pointing, and almost three quarters of the time was spent at just three locations (Law et al., 2015). It is possible that pointing-to-pointing event rate variance contributed to their not seeing anything.

We therefore warn that deep surveys are at a disadvantage to those that sweep large regions of the sky (CHIME (Bandura, 2014), UTMOST[1], HIRAX) because the non-

---

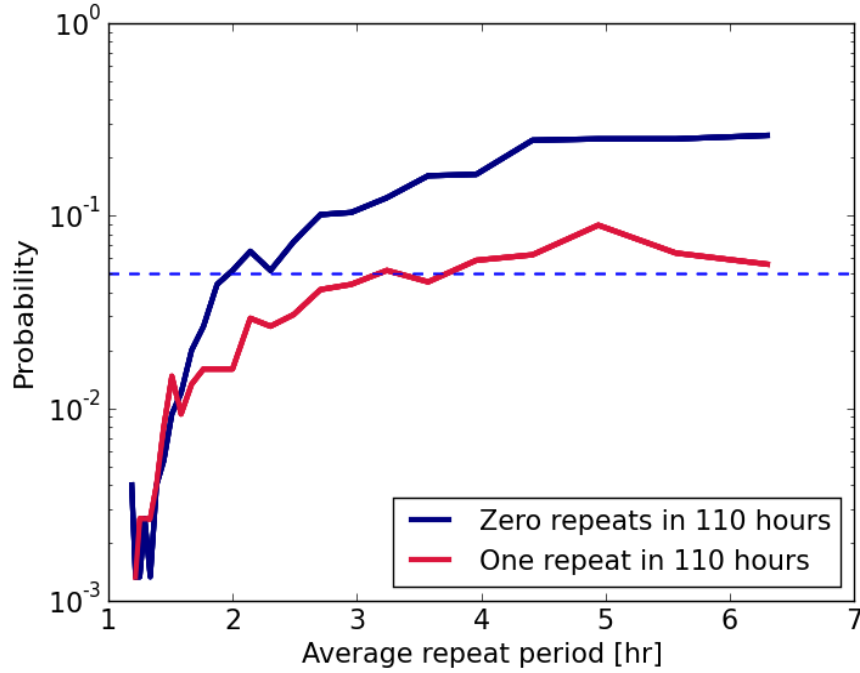[1]http://www.caastro.org/news/2014-utmost

Figure 1.2: The probability of seeing zero (blue curve) or one (red curve) repeat burst in 110 hours of follow-up, assuming a $1/f$ distribution. The curves are derived from a simple Monte Carlo in which a pink distribution was generated with one sample per hour, and we asked how many bursts were seen in 110 samples. Thousands of 110-hour realizations were then averaged for each repeat period, $P$. Even with an average repeat rate of once every two hours, there is still a 5% chance (indicated by the dashed line) of seeing one or fewer bursts, despite the expected value of 55.

repeating scenario is unaffected; whereas shallow observations should not hurt the detection rate, no matter what their repetition. Ideally, a survey needs only to spend a few dispersion delay times on each beam before moving on.

## 1.4 FRB 110523 and sub-L-band statistics

To date, estimating the all-sky rate of FRBs has proven difficult, even at 1.4 GHz where most have been found (Lorimer et al., 2007a; Keane et al., 2012; Thornton et al., 2013a; Petroff et al., 2015a; Champion et al., 2015a; Spitler et al., 2014a). This is in part because of their unknown flux distribution and location within the radio telescope beam, as well as the low number of observed events. It is further exacerbated by the different specifications of the surveys that find them, whose disparate search algorithms, fluence completenesses, and sensitivity can affect their detection rate. Extrapolating to other

frequencies is also difficult since spectral indices and the extent of scattering are still unknown.

Thornton et al. (2013a) searched about 25% of the High Time Resolution Universe (HTRU) survey data and found four FRBs. They estimated an all-sky daily rate of $1.0^{+0.6}_{-0.5} \times 10^4$ above $\sim 3$ Jy ms from 23 days of data and using a 0.55 deg$^2$ beam. The rate based on HTRU has since come down ($6^{+4}_{-3} \times 10^3$ sky$^{-1}$ day$^{-1}$) with the discovery of five more FRBs in three times as much data (Champion et al., 2015a). Keane & Petroff (2015) also found a rate that was lower than the initial estimate, calculating $\sim 2500$ sky$^{-1}$ day$^{-1}$ after accounting for completeness factors like fluence sensitivity. Though the error bars are still significant, there is some convergence on the rate, and it now seems likely that there are thousands of such events each day at 1.4 GHz.

Event rate estimates at 1.4 GHz are converging, but strong rate constraints have not yet been made in other bands. The non-detection by UTMOST (an upgrade to the Molonglo Observatory Synthesis Telescope) (Caleb et al., 2016b) placed a $2\sigma$ upper limit on the number of bright events ($10^3$ events per sky per day above 11 Jy ms) after searching 467 hours at a fraction of its eventual sensitivity. FRB 110523 remains the only published event not found around 1.4 GHz. It was found near 800 MHz, where scattering or the intrinsic spectral index might have rendered this lower-frequency FRB unobservable. Kulkarni et al. (2015) argued that the steep blue spectrum seen in FRB 121102 (Spitler et al., 2014a) was indicative of free-free absorption, the optical depth of which scales as $\lambda^{2.1}$ and would make metre-wave bursts difficult to see. A greater concern comes from scattering. Sources broadened by scattering to $\sim 10$ ms at 1.4 GHz would be $\sim 100$ ms at 800 MHz, and a couple of seconds at 400 MHz, due to the $\lambda^4$ scaling of the scattering width.

Some surveys that could have great impact on FRB science are threatened by strong scattering. ALERT hopes to localize dozens of bursts with LOFAR after finding them with the large field-of-view (FoV) APERTIF (van Leeuwen, 2014; Verheijen et al., 2008), UTMOST will have $\sim 8$ deg$^2$ of sky coverage 24/7 at 843 MHz (Caleb et al., 2016b), and HIRAX[2], Tianlai[3] and CHIME (400-800 MHz) could see $10^{2-4}$ per year, with the ability to write full polarization information (Bandura, 2014). However, their success depends on whether or not the rate of detectable FRBs is comparable to that at higher frequencies.

---

[2]http://www.acru.ukzn.ac.za/~hirax/
[3]http://tianlai.bao.ac.cn/

### 1.4.1 Implications for the flux distribution

FRB 110523 was found by searching data from the Green Bank Hydrogen Intensity Mapping (GBTIM hereon) survey (Chang et al., 2010; Masui et al., 2015a; Switzer et al., 2013). These data were taken with $1.024\,\mathrm{ms}$ cadence between 700-900 MHz using the GBT linearly-polarized prime-focus $800\,\mathrm{MHz}$ receiver, along with the GBT Ultimate Pulsar Processing Instrument (GUPPI) digital back-end. An effective DM range of 20-$2000\,\mathrm{pc\,cm^{-3}}$ was then searched for FRBs. At each DM, the data were convolved with all possible lengths of top-hat windows up to $100\,\mathrm{ms}$ to search for peaks. The peaks were then compared to the root mean square (RMS) of the convolved time-stream, the ratio of which is what we will refer to as signal-to-noise ratio (SNR). The survey duration was 660 hours.

In order to test the observed FRB flux distribution, $N(F)$, we can apply a standard $\log(N)$-$\log(F)$ test. We will consider only power-law distributions of form $N(>F) \propto F^{-\gamma}$. In a Euclidean Universe a population of sources that are uniformly distributed in space should have $N(>F) \propto F^{-3/2}$. This makes intuitive sense, since number counts ought to increase like the cube of distance, while the flux falls off as inverse squared distance.

With no FRBs found between the search algorithm's detection threshold, $8\sigma$, and $32\sigma$, where FRB 110523 was found, we can test if this has any implications for the true flux distribution. The question we are trying to answer is "Having seen a single event, what is the probability that it has SNR greater than $s$ for a given value of $\gamma$?". This is given by the ratio of integrals,

$$\beta \equiv \frac{\int_{s_{\max}}^{s_\infty} N(s)ds}{\int_{s_{\min}}^{\infty} N(s)ds}, \tag{1.2}$$

which reduces to $\beta = \left(\frac{s_{\max}}{s_{\min}}\right)^{-\gamma}$ for $\gamma \neq 0$ and integrands of the form $N(s) \propto s^{-\gamma-1}$. This statistic is equivalent to the $V/V_{\max}$ test that has been used to probe the underlying spatial distribution of quasars (Schmidt, 1968a) as well as gamma-ray bursts (Ogasaka et al., 1991). Calculating $\beta$ as a function of $\gamma$ shows that steep distributions with $\gamma > 2.2$ are ruled out with 95% confidence by this single detection alone.

This is mathematically equivalent to the single-burst solution to a more general approach similar to the biased coin-flip scenario outlined by Connor et al. (2016e). If $M_{\mathrm{high}}$ FRBs are observed above a threshold SNR of $s_{\mathrm{thresh}}$, with $M_{\mathrm{tot}}$ above $s_{\min}$, and $p$ is the relative probability of detecting an FRB in the high-SNR region, then

$$P(M_{\mathrm{high}} | M_{\mathrm{tot}}, p) = \binom{M_{\mathrm{tot}}}{M_{\mathrm{high}}} p^{M_{\mathrm{high}}} (1-p)^{M_{\mathrm{tot}} - M_{\mathrm{high}}}, \tag{1.3}$$

where $p$ is just $\beta(\gamma)$. Clearly this reduces to the previous result in the case where $M_{\text{high}} = M_{\text{tot}} = 1$.

### 1.4.2 How to discuss event rate

The simplest constraints one can make, given a set of observations, will be an expected event rate for a future survey with identical parameters. Transferring that rate to another survey or onto the sky requires care, and in both cases uncertainties are introduced that are hard to quantify. For this reason we start by calculating a rate for GBTIM in Sect. 1.4.3, which predicts how many FRBs are expected if an identical survey were to take place again. After that we discuss the implications for other comparable surveys, which should be fairly robust against things like burst-width sensitivity and the choice of fluence thresholds. In Sect. 1.4.5 we provide an all-sky rate, with several caveats, and discuss the meaning of such a value.

### 1.4.3 Burst rate

The rate of FRBs implied by 110523 will be independent of its observed brightness. The relevant quantity is the survey sensitivity, so $s_{\text{min}}$ is the only flux scale that should show up in our rate estimate. For a true rate $\mu_0$ above $s_{\text{min}}$, we would expect the number of bursts, $M$, in a given survey above some SNR, $s$, to be

$$M_s = \mu_0 \, \Omega \, T_{\text{int}} \frac{N(>s)}{N(>s_{\text{min}})}, \tag{1.4}$$

where $\Omega$ is the telescope's FoV and $T_{\text{int}}$ is the time on sky. We use the rate above some SNR so that we can easily scale it to a rate prediction for a different survey without making any implicit assumption about the distribution of FRBs in flux, fluence, or duration. Similar to Eq. (1.2), this becomes

$$M_s = \mu_0 \, \Omega \, T_{\text{int}} \frac{s^{-\gamma}}{s_{\text{min}}^{-\gamma}} \quad \text{for } \gamma > 0. \tag{1.5}$$

However, since we will not try to estimate an all-sky daily rate until Sect. 1.4.5, for now we will take $T_{\text{int}}$ and $\Omega$ to be in units of the GBTIM on-sky time and beam-size. Therefore $M_s$ should be thought of as the number of FRBs one would expect if the GBTIM were repeated.

**Frequentist rate limits**

If we regard the sky rate $\mu_0$ as fixed, we can immediately write down the probability of observing $M_{\text{tot}}$ FRBs above a SNR of $s$. It is simply given by the Poissonian distribution

$$P(M_{\text{tot}}|\mu_0) = \frac{M_{s_{\min}}^{M_{\text{tot}}} \mathrm{e}^{-M_{s_{\min}}}}{M_{\text{tot}}!}, \tag{1.6}$$

where $M_{s_{\min}}$ is given by Eq. (1.5) for $s = s_{\min}$. Now we can ask which values of $M_s$ make the observed value of $M_{\text{tot}} = 1$ unlikely. Choosing a threshold value of 5%, we can—in this sense—rule out expected event counts $M_{s_{\min}}$ outside of the range from 0.05-4.50 events per GBTIM-like survey, with a maximum likelihood value at 1.

**Bayesian rate limits**

From a Bayesian viewpoint, we want to look at the posterior for the expected number of detections, $M_{s_{\min}}$ rather than the likelihood. For simplicity we choose a flat prior on $M_{s_{\min}}$, which means that the posterior is again

$$\mathcal{P}(M_{s_{\min}}|M_{\text{tot}}) = \frac{M_{s_{\min}}^{M_{\text{tot}}} \mathrm{e}^{-M_{s_{\min}}}}{M_{\text{tot}}!}. \tag{1.7}$$

Note that, although the posterior has the same functional form as the likelihood, it is to be read as a density in $M_{s_{\min}}$ rather than a probability for $M_{\text{tot}}$. Now we can calculate another 95% confidence interval, defined as the smallest interval $I$ with the property $\int_I \mathrm{d}\mu_0 \, \mathcal{P}(\mu_0|M_{\text{tot}}) = 0.95$. We find for this 95% confidence interval $I = [0.24, 5.57]$ events for a GBTIM-like survey. From hereon we will quote the rate error bars based on the posterior. The posterior for $\mu_0$, which is the same as Eq. (1.7) multiplied by $\Omega \, T_{\text{int}}$, is shown in Fig. 1.3.

## 1.4.4   Implications for other surveys

Though only one event was observed in the 660 hours of archival data, the fact that any burst was detectable in this band is significant. Some of the most important upcoming surveys for FRB science will observe below 1.4 GHz. UTMOST (Caleb et al., 2016b) will be on the sky 24/7 with an $\sim 8$ deg$^2$ FoV and 18,000 m$^2$ of collecting area, observing at 843 MHz. ALERT hopes to localize dozens of FRBs by first detecting them with the large-FoV APERTIF (van Leeuwen, 2014; Verheijen et al., 2008) and then following up with roughly arcsecond resolution when they arrive several minutes later at LOFAR. Another survey for which FRB 110523's discovery is relevant is CHIME, observing at 400-

800 MHz. If the event rate in this band is comparable to the one at higher frequencies, then its large FoV and uninterrupted observing will make it by far the fastest FRB survey.

Since the rate of detection depends on an interplay of the underlying FRB flux and scattering distributions with a survey's thermal sensitivity, fluence completeness, and observing frequencies, the comparison of two surveys with similar specifications is by far the safest bet. CHIME has $\sim 8,000$ m$^2$ of collecting area compared to GBT's $\sim 7,850$ m$^2$ and has 100 MHz of overlap with GBTIM. UTMOST will observe within the GBTIM band with similar sensitivity per steradian. Though others (Burke-Spolaor & Bannister, 2014a) have provided models for calculating inter-survey sensitivity based on sky pointing and temporal broadening, we compare only similar telescopes and adopt the simplest possible comparison based on known features of each instrument. Given how little is known about scattering properties and spectral indices, we provide only a skeleton model below; a more detailed calculation is beyond the scope of this paper.

A survey, $\Sigma$, that is similar to the GBTIM experiment will see $N_\Sigma$ events per day based on the one detected burst in $\sim 27.5$ days at GBT. This is given by

$$N_\Sigma = \frac{1}{27.5} \left( \frac{G_\Sigma}{G_{\text{GBT}}} \frac{\langle T_{\text{GBT}}^{\text{sys}} \rangle}{\langle T_\Sigma^{\text{sys}} \rangle} \sqrt{\frac{B_\Sigma}{B_{\text{GBT}}}} \right)^\gamma \left( \frac{\Omega_\Sigma}{\Omega_{\text{GBT}}} \right) \text{ day}^{-1} \qquad (1.8)$$

where $B$ gives the survey's bandwidth, $G$ is the gain, and $\langle T^{\text{sys}} \rangle$ gives the pointing-averaged system temperature. For GBT we take the effective solid angle based on the full-width half max (FWHM) in power, giving $\Omega_{\text{GBT}} \sim 0.055$ deg$^2$. We use 26.5 K for the sky-averaged system temperature, and a gain of 2 K Jy$^{-1}$.

As discussed above, in assessing the impact FRB 110523's detection on other surveys, we want to avoid venturing into the unknown. For this reason we consider only the 100 MHz of overlap between CHIME and GBTIM, since that region is known to have a non-zero rate of observable FRBs. For things like beam size, we take the maximum possible FoV based on CHIME's optics and let others adjust the effective solid angle accordingly; though the CHIME collaboration may search only a subset of their primary beam in order to optimize other aspects of their FRB survey, we will estimate the rate based on a full beam.

We model CHIME's primary beam at 750 MHz based on Shaw et al. (2015). A simple dipole beam in the aperture plane is propagated onto the sky by treating the reflector along the cylinder (north-south direction) as a mirror, and by solving the Fraunhofer diffraction problem in the east-west direction. As with GBT, we use only the beam within the half-max contour. This gives $\Omega_{\text{CH}} \sim 86$ deg$^2$ in the middle of its band

compared to $\Omega_{\rm GBT} \sim 0.055$ deg$^2$. Though this gives a ratio of $\sim 1600$ between the two telescope's beam sizes, we remind the reader that this is an approximate solid-angle upper-limit for CHIME between 700-800 MHz. We then estimate its aperture efficiency as 50%, compared with 72% at GBT[4], whose feed horn maximally illuminates its dish while minimizing ground spill, something that is difficult with CHIME's dipole antennas. This makes $G_{\rm CH} = 1.38$ K Jy$^{-1}$. Finally, keeping with 26.5 K for GBT's system temperature as before and using CHIME's design system temperature of 50K (Bandura, 2014), we can write the maximum-likelihood value for the CHIME rate as

$$N_{\rm CH} \approx 7.5 \left( \frac{50\,{\rm K}}{T^{\rm sys}} \right)^{1.5} {\rm day}^{-1} \tag{1.9}$$

assuming a Euclidean distribution. This means with a 50 K system temperature, CHIME could see between 2-40 (95%) bursts per day if it searches its whole FoV, based on the known non-zero rate above 700 MHz. With a more conservative sky-averaged system temperature $T^{\rm sys} = 100$ K, CHIME might expect between one every couple of hours and one every two days.

Caleb et al. (2016b) estimate the daily rate of UTMOST in a similar way, directly comparing their sensitivity with that of Parkes at 1.4 GHz. They estimate that they will see a burst once every several days. However, with our constraints on the rate between 700-900 MHz, we can recompute UTMOST's detection rate based on the same band, once it reaches final sensitivity. We use $G = 3.6$ K Jy$^{-1}$, $T^{\rm sys} = 70$ K, $B = 31.25$ MHz, and a factor of $1/\sqrt{2}$ for its single polarization, based on Caleb et al. (2016b). This gives $4.2^{+19.6}_{-3.2} \times 10^{-1}$ day$^{-1}$, or between a couple per day and one every couple of weeks. This is consistent with Caleb et al. (2016b).

Finally, we estimate rates for three smaller telescopes related to CHIME. We use $\gamma = 3/2$ and only the 100 MHz of overlap bandwidth with GBTIM, as before. CHIME's Pathfinder, which is made of two 20×37 metre cylinders, has been commissioned over the last two years and now has a working beamforming back-end. If the single formed beam were on sky searching for FRBs at all times, one might expect to detect $0.4 - 9$ per year, taking its beam to be $\Omega_{\rm PF} = 0.62$ deg$^2$ and $G_{\rm PF} = 0.26$ K Jy$^{-1}$. The 26 m John A. Galt Telescope, just $\sim 150$ m from the CHIME Pathfinder at the Dominion Radio Astrophysical Observatory (DRAO), could detect $0.1 - 3$ each year, with $\Omega_{26} = 0.78$ deg$^2$ and $G_{26} = 0.09$ K Jy$^{-1}$. Another telescope to which a simple FRB back-end could be attached is the 46 m Algonquin Radio Observatory (ARO). This might yield $0.2 - 4.5$ per year, using $\Omega_{\rm ARO} = 0.25$ deg$^2$ and $G_{\rm ARO} = 0.29$ K Jy$^{-1}$. Though none of these telescopes

---

[4]https://science.nrao.edu/facilities/gbt/proposing/GBTpg.pdf

makes for a very fast survey, the cost of searching is quite small, and a coincident detection between DRAO and ARO could provide a sub-arcsecond localization.

### 1.4.5 All-sky daily rate

The standard method for estimating an all-sky rate given a set of observations is to first calculate the rate, $\mu_0$, for that survey — usually the observed number of FRBs divided by the beam size and the time on sky — and then to scale that based on the survey's sensitivity threshold and a flux distribution index, $\gamma$. This threshold has typically been in fluence, a physically motivated quantity for FRBs, and is given by

$$H_{\min} = \frac{s_{\min} \langle T^{\text{sys}} \rangle \tau}{G\sqrt{m\tau B}}, \tag{1.10}$$

where $\langle T^{\text{sys}} \rangle$ is the pointing-averaged system temperature, as before, $s_{\min}$ is the SNR threshold used in the search algorithm, $G$ is the gain at beam centre, $B$ is the bandwidth, $m$ gives the number of polarizations, and $\tau$ is some timescale. If one then wants to quote the rate above, say, $3\,\text{Jy}\,\text{ms}$, then the rate becomes $\mu \times \left( \frac{H_{\min}}{3\,\text{Jy}\,\text{ms}} \right)^{\gamma}$.

One problem with this method is that it is not entirely obvious how to choose $\tau$, and several groups have approached it differently. Keane & Petroff (2015) discuss some of these effects and decided to use the value at which their survey becomes fluence complete, $2\,\text{Jy}\,\text{ms}$, based on the maximum width to which they are sensitive. Rane et al. (2016) use sampling time, which is the minimum possible effective burst width. This will maximise the reported search sensitivity because it uses the lowest possible fluence limit, and therefore generically lowers the final rate estimate after scaling to a common fluence. A more exact approach is to quote the rate above some fluence curve $H \propto \sqrt{\tau}$ between $\tau_{\min}$ and $\tau_{\max}$ corresponding to the actual SNR threshold if white noise is assumed. This is similar to what Champion et al. (2015a) do, who quote their rate above a fluence range.

Since the primary goal of this paper is to compare between surveys, we do not attempt to derive a strict fluence threshold for GBTIM and to scale our all-sky rate based on it. Until the fluence and width distributions for FRBs are known along with a search algorithm's width response, the all-sky rate quoted for some incomplete region of fluence space is not overly useful. Instead, we calculate the rate above our true threshold, which is $s_{\min} = 8$ for DMs between 20-2000 $\text{pc}\,\text{cm}^{-3}$ and widths between one and two hundred milliseconds. A useful estimate of the rate is given by the maximum of Eq. (1.7), $\mu_0 = \frac{1}{\Omega\,T_{\text{int}}} \left( \frac{s}{s_{\min}} \right)^{\gamma}$, for $s = s_{\min}$. The all-sky rate for GBTIM above $8\sigma$ is then $2.7^{+12.4}_{-2.1} \times 10^4\,\text{sky}^{-1}\,\text{day}^{-1}$, between 700-900 MHz. We plot the corresponding posterior in Fig. 1.3.
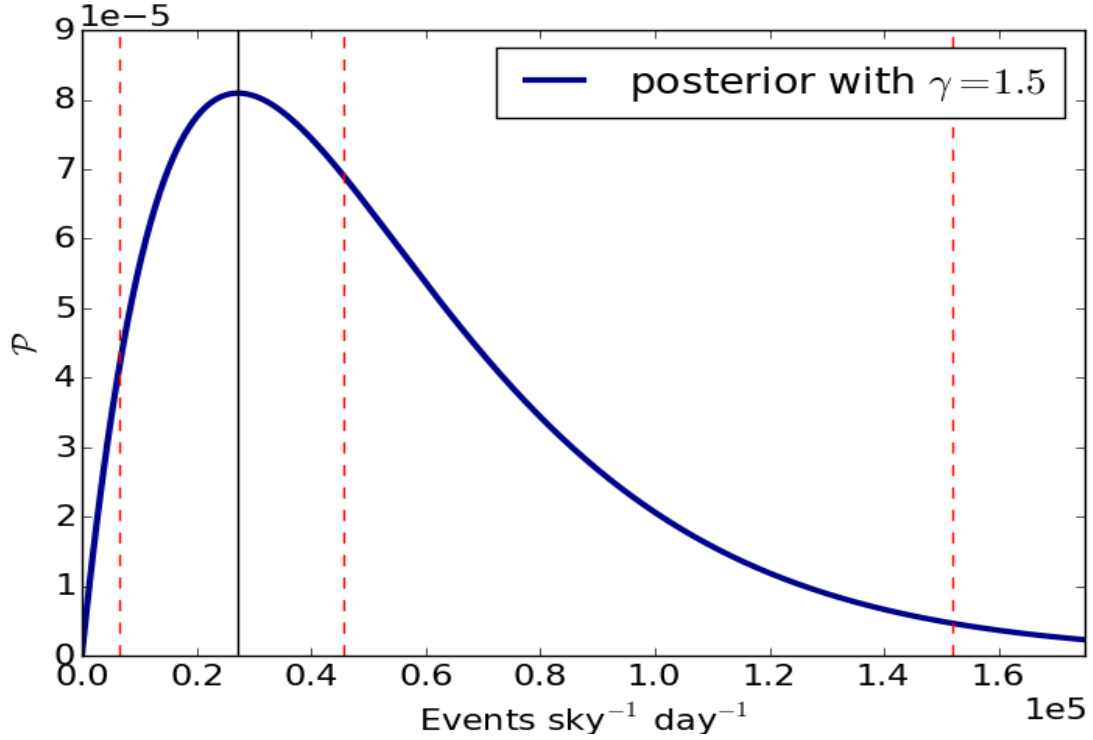
Figure 1.3: Posterior distribution for the all-sky daily rate based on seeing one burst in 27.5 days of data with a $0.055\,\mathrm{deg}^2$ beam. This posterior is meant to be interpreted as the number of FRBs one would see if GBTIM-like surveys were able to observe the whole sky for a day, i.e. we have not scaled the rate based on fluence sensitivity for reasons described in Sect. 1.4.5. The maximum a posteriori value is denoted by the black vertical line, which is at $\sim 2.7 \times 10^4\,\mathrm{sky}^{-1}\,\mathrm{day}^{-1}$. The two outside blue lines enclose 95% of the curve and the middle blue line denotes the median.

Though this value seems high, GBTIM is a sensitive survey, with $F_{\min} = 97\,\mathrm{mJy}$ for a 3 ms pulse. Without making any concrete statements about our sensitivity in fluence space, we can get an idea of how this rate compares to the estimates from other surveys based only on thermal sensitivity. We can use the rate inferred from the 9 HTRU FRBs as a baseline (Champion et al., 2015a). If we assume the width completeness of various surveys is roughly similar, we can tether our rate to the HTRU one, and calculate a sensitivity ratio, $r_s$. Comparing Parkes and GBT, this will be

$$r_s = \frac{\langle T_{\mathrm{H}}^{\mathrm{sys}} \rangle}{\langle T_{\mathrm{GBT}}^{\mathrm{sys}} \rangle} \frac{G_{\mathrm{GBT}}}{G_{\mathrm{H}}} \sqrt{\frac{B_{\mathrm{GBT}}}{B_{\mathrm{H}}}} \frac{s_{\min}^{\mathrm{H}}}{s_{\min}^{\mathrm{GBT}}}. \tag{1.11}$$

Using $s_{\min}^{\mathrm{H}} = 10$, an average on-axis gain of $G_{\mathrm{H}} = 0.64\,\mathrm{K\,Jy}^{-1}$, $B_{\mathrm{H}} = 340\,\mathrm{MHz}$, and a 23 K system temperature (Keith et al., 2010a), we find $r = 2.60$. Our rate can then by

multiplied by $r^{-\gamma}$, which gives $6.4^{+29.5}_{-5.0} \times 10^3 \, \mathrm{sky}^{-1} \, \mathrm{day}^{-1}$, assuming a Euclidean distribution.

This is an extrapolation of our rate estimate at 700-900 MHz to 1.4 GHz. It corresponds to the number of FRBs that HTRU should be detecting if the intrinsic rates of FRBs in the two frequency bands were the same. This extrapolated rate is indeed consistent with the rate observed by HTRU, which shows that the rate of FRBs detectable at low frequencies is not significantly lower than at 1.4 GHz, which was not previously obvious due to the threat of scattering and steep blue power-laws (Kulkarni et al., 2015). This result makes the aforementioned upcoming low-frequency surveys especially promising for FRB science.

This is also consistent with the non-detection upper-limit set by Caleb et al. (2016b), who found the rate to be below $10^3 \, \mathrm{sky}^{-1} \, \mathrm{day}^{-1}$ for one-millisecond 11 Jy bursts at the $2\sigma$ level. This was based on two surveys, one with 467 hours on sky, and another with 225 hours on sky at roughly twice the sensitivity. Comparing their time-weighted thermal sensitivity with GBTIM, we get $r_s \approx 10^2$, making our 95% upper-limit a few hundred per sky per day.

## 1.5   Latitudinal dependence

There is now evidence that the FRB rate is nonuniform on the sky, with fewer detectable events at low Galactic latitudes (Burke & Graham-Smith, 2014). However the statistical significance of this finding may be overestimated. Petroff et al. (2014) compute the probability of the disparity between the number of bursts seen in the high- and intermediate-latitude ($|b| < 15°$) components of the High Time Resolution Universe survey (HTRU). They calculate the probability of seeing $N = 0$ in the intermediate latitude survey and $M = 4$ in the high-latitude, despite having searched 88% more data in the former, and they rule out the uniform sky hypothesis with 99.5% certainty. We would point out that in general $P(N|M)$ describes a very specific outcome, and it would be more appropriate to include all outcomes equally or more unlikely. That number might also be multiplied by two, since if the survey found four intermediate-latitude FRBs and zero high-lat ones, we would ask the same question.

But a simpler approach to this problem would be analogous to a series of coin flips. If a coin were flipped four times, the probability of seeing all heads is 1/16, or 6.25%. This is a factor of six higher than the analogous analysis of Petroff et al. (2014). We can test the null hypothesis that the coin is fair, and using the binomial statistic would conclude that the outcome is consistent with a fair coin at 95% confidence, differing from the

conclusion of Petroff et al. (2014). In the FRB case the Universe is flipping a coin each time a new burst appears, with some bias factor due to things like different integration times. HTRU has since reported five more bursts in the high Galactic region, but using a dataset that spent ∼2.5 times more time at high latitudes. Below we try and quantify the likelihood of this.

If one wants to compare two statistical hypotheses, then the claims of each should be treated as true and their likelihood discrepancy should be computed. In the case of testing the abundance of FRBs at high latitudes, the sky should be partitioned into high and low regions a priori (e.g., the predefined high-latitude HTRU and its complement). The rate in both regions is then taken to be the same, and the likelihood of a given spatial distribution of observed sources can be calculated. This situation is naturally described by a biased binomial distribution with a fixed number of events. Suppose a total of $K$ FRBs are observed in a given survey. We can ask the question, what is the probability of seeing $M$ events in the high region and $(K - M)$ events in the lower region? This probability can be calculated as

$$P(M \,|\, K, p) = \binom{K}{M} p^M (1 - p)^{K-M}, \tag{1.12}$$

where $p$ is the probability that an event happens to show up in the high region. In a survey where more time is spent on one part of the sky than the other, $p = \alpha/(\alpha + 1)$, where $\alpha$ is the ratio of time spent in the high-latitude region vs. the intermediate region. In the case of the HTRU survey, $K = 9$ and since none were found in the low-latitude region, $M = 9$. Roughly 2500 hours were spent searching the upper region and ∼ 1000 hours were spent at $|b| < 15°$, giving $\alpha = 2.5$. Using Equation 1.12, this outcome is only ∼ 5% unlikely.

The problem is given a quasi-Bayesian treatment by Petroff et al. (2014), which gives the following.

$$P(N \,|\, M) = \alpha^N (1 + \alpha)^{-(1+M+N)} \frac{(M + N)!}{M! N!} \tag{1.13}$$

This gives a probability of ∼3.5%, using all nine FRBs. This method is Bayesian in the sense that they marginalize over the unknown rate and calculate a likelihood, but they then calculate a confidence and do not look at a posterior.

The most obvious difference between the approach we have offered (biased coin-flip) and the quasi-Bayesian method is that we take $M + N$ to be fixed. It follows to ask whether or not we *should* regard the total number of FRBs as "given"? We believe the answer is yes, since this is one of the few quantities that we have actually measured,

along with $M$ and $N$. What we are really trying to infer is how much larger $\mu_{\text{high}}$ is than $\mu_{\text{low}}$, so these rates should not be marginalized over.

To consider only the likelihood can give misleading results. For example, as more and more FRBs are detected, the likelihood of the particular observed values for $N$ and $M$ will become smaller and smaller, due to the sheer number of possible tuples $(N, M)$. To decide whether or not there is evidence for FRBs to occur with a higher probability at high latitudes, we can instead use the formalism of Bayesian model selection. This formalism does not aim to rule out a particular model, it only compares the validity of two models. For this, we formulate two specific models, Model 1 in which we assume that $p_1 = \alpha/(1 + \alpha)$ as above (i.e. uniform rate across the sky), and Model 2 in which we regard $p$ as a free parameter, equipped with a flat prior between 0 and 1. The model selection will then be based on the comparison of the posterior probabilities for the two models,

$$\frac{P(\text{Model } 1|M, K)}{P(\text{Model } 2|M, K)} = \frac{P(M|\text{Model } 1, K)}{P(M|\text{Model } 2, K)}, \tag{1.14}$$

where we have assumed equal prior weights for the two models. Using the binomial likelihood, Eq. (1.12), and marginalizing over the unknown probability $p$ in the case of Model 2, this ratio is easily calculated to be

$$\frac{P(M|\text{Model } 1, K)}{P(M|\text{Model } 2, K)} = (K + 1) \binom{K}{M} p_1^M \, (1 - p_1)^{K-M} . \tag{1.15}$$

For the observations discussed above with $M = K = 9$ and $\alpha = 2.5$, we find a ratio of 0.48, so there is no strong preference for either of the two models.

## 1.6 Is the distribution Euclidean?

In the simple constant-density Euclidean model, the power-law behaviour of Eq. (??) is not only valid for the flux densities, but also for any other observable that depends linearly on flux density. One example would be the fluence

$$F = \int \mathrm{d}t \, S(t)$$
$$= S \, \tau, \tag{1.16}$$

where $\tau$ is the duration of a burst and $S$ is the average flux density within the interval of length $\tau$. Another example is the observed signal-to-noise ratio, which depends on the

flux density of the burst, its duration, and of course on properties of the telescope and the survey. In many cases it can be approximated as

$$s \approx K \, S \, \tau^{1/2}, \tag{1.17}$$

where we include all instrumental properties in the constant $K$ (e.g., Caleb et al., 2016a). The detection of an FRB is always subject to a sensitivity cutoff in signal-to-noise, and not in flux density or fluence. This makes the statistics of flux density and fluence more complicated than the statistics of the signal-to-noise ratio $s$ and we choose to cast all equations in terms of $s$. Note that, as is common in the field, we use the term signal-to-noise ratio to mean the amplitude of the FRB signal plus noise, divided by the standard deviation of the noise, which can be approximately determined empirically for each search window length $\tau$.

We derive the necessary statistical methodology in the following section, discuss the data that we use and show our results in Sect. 1.8. We conclude with a discussion in Sect. **??**.

## 1.7   Methodology

### 1.7.1   Likelihood for the observed signal-to-noise ratios

Clearly some information on the parameter $\alpha$ is contained in the distribution of observed signal-to-noise ratios. If we assume a value for $\alpha$ and suppose that a survey with a given signal-to-noise threshold $s_{\min}$ detects an FRB, then the likelihood for its signal-to-noise ratio to be $s$ is, according to Eq. (**??**),

$$\mathcal{P}(s|s_{\min}, \alpha) = \begin{cases} \frac{\alpha}{s_{\min}} \left(\frac{s}{s_{\min}}\right)^{-(\alpha+1)} & \text{if } s \geq s_{\min} \\ 0 & \text{else} \end{cases}. \tag{1.18}$$

If the survey detects $n$ independent FRBs then the joint likelihood for their signal-to-noise ratios is simply the product of the individual ones.

For $N$ different surveys, each detecting $n_1, \ldots, n_N$ FRBs, the situation is the same, except that we have to take into account that each survey has a different detection threshold $s_{\min}$. If we denote the observed signal-to-noise value of the $i$-th FRB in the $I$-th survey as $s_{I,i}$, the $(n_1 + \cdots + n_N)$-dimensional vector of all these observed values as $\vec{s}$, the $N$-dimensional vector of all threshold signal-to-noise values as $\vec{s}_{\min}$, and the $N$-dimensional vector of the numbers of detections in each survey as $\vec{n}$, the complete

likelihood becomes

$$\mathcal{P}(\vec{s}|\vec{n}, \vec{s}_{\min}, \alpha) = \prod_{I=1}^{N} \prod_{i=1}^{n_I} \mathcal{P}(s_{I,i}|s_{\min,I}, \alpha). \tag{1.19}$$

This is easily calculated and we will do so in Sect. 1.8. In the following we will refrain from mentioning $\vec{s}_{\min}$ explicitly in the notation of probabilities and imply that all survey properties are always fixed.

Note that the combination $(s/s_{\min})^{-\alpha}$ for $\alpha = 3/2$ corresponds to the ratio of the volume interior to the FRB and the volume in which this particular FRB could have been detected by the survey, $V/V_{\max}$, for a constant source density in three-dimensional Euclidean space. The likelihood we are using here to constrain $\alpha$ is thus closely related to the $V/V_{\max}$-test used in many contexts to check for deviations from a constant density for a source population (e.g., Schmidt, 1968b).

## 1.7.2 Likelihood for the number of observed FRBs

In addition to the information contained in the signal-to-noise ratios of the observed bursts, some information is also contained in the numbers of bursts detected by different surveys. For any one survey, the number of detected FRBs puts constraints on the rate of FRBs occurring above the detection threshold of that survey. This rate can be rescaled to a different survey with a different detection threshold and confronted with the observed number of bursts for that survey. However, the rescaling depends on the parameter $\alpha$ and thus the number of bursts detected by two or more surveys puts constraints on $\alpha$.

To include these constraints in our analysis we introduce the FRB rate explicitly as an unknown parameter. Since the rate observable by a given survey depends on various properties of the survey, we define the rate $r_0$ occurring above the detection threshold of a hypothetical survey described by a system temperature $T_{\mathrm{sys},0} = 1\,\mathrm{K}$, a gain $G_0 = 1\,\mathrm{K\,Jy^{-1}}$, $n_{\mathrm{p},0} = 2$ observed polarizations, a bandwidth $B_0 = 1\,\mathrm{MHz}$, and a signal-to-noise threshold $s_{\min,0} = 1$. As explained by Connor et al. (2016b), the FRB rate above the detection threshold of the $I$-th survey is then a rescaled version of this rate, namely

$$\begin{aligned} r_I &= r_0 \left( \frac{T_{\mathrm{sys},I}}{T_{\mathrm{sys},0}} \frac{G_0}{G_I} \sqrt{\frac{n_{\mathrm{p},0}\,B_0}{n_{\mathrm{p},I}\,B_I}} \frac{s_{\min,I}}{s_{\min,0}} \right)^{-\alpha} \\ &= r_0 \left( \frac{T_{\mathrm{sys},I}}{G_I} \sqrt{\frac{2\,\mathrm{MHz}}{n_{\mathrm{p},I}\,B_I}}\, s_{\min,I}\,\mathrm{Jy} \right)^{-\alpha}. \end{aligned} \tag{1.20}$$

The expected number of FRBs detected by the $I$-th survey will then be

$$M_I = r_I \, \Omega_I \, T_I, \tag{1.21}$$

where $\Omega_I$ is the angular size of the survey's field of view and $T_I$ is the time spent surveying. The likelihood for the actual number of FRBs observed in this survey is then a Poissonian distribution with this expectation value,

$$P(n_I|r_0, \alpha) = \frac{M_I{}^{n_I}}{n_I!} \, \mathrm{e}^{-M_I}. \tag{1.22}$$

For $N$ surveys the complete likelihood again becomes a product of the likelihoods for the individual surveys,

$$P(\vec{n}|r_0, \alpha) = \prod_{I=1}^{N} P(n_I|r_0, \alpha), \tag{1.23}$$

and can be used to put constraints on the distribution of flux densities via the parameter $\alpha$, as well as on the overall rate of FRBs, here parameterized as the rate above the detection threshold of our hypothetical survey, $r_0$.

### 1.7.3  Posterior

To get the complete set of constraints on the distribution of flux densities, both from the observed signal-to-noise ratios and from the detection numbers of different surveys, we combine the results of Sects. 1.7.1 and 1.7.2. We write the joint likelihood for the number of observed FRBs and their signal-to-noise ratios as

$$\begin{aligned}
\mathcal{P}(\vec{s}, \vec{n}|r_0, \alpha) &= \mathcal{P}(\vec{s}|\vec{n}, r_0, \alpha) \, P(\vec{n}|r_0, \alpha) \\
&= \mathcal{P}(\vec{s}|\vec{n}, \alpha) \, P(\vec{n}|r_0, \alpha).
\end{aligned} \tag{1.24}$$

If we assume flat priors for $r_0$ and for $\alpha > 0$, this likelihood is proportional to the joint posterior for the parameter $\alpha$ and the rate $r_0$.

The likelihood for observed fluxes within a survey obviously only gives us constraints if the survey has in fact detected at least one FRB. Note, however, that we can in principle include surveys without FRB detection by setting

$$\mathcal{P}(\vec{s}|n = 0, s_{\min}, \alpha) = 1 \tag{1.25}$$

and thus still use them to constrain the parameter $\alpha$ via their implications on the FRB

rate above their detection thresholds. Similarly, the numbers of FRBs detected by different surveys only have implications for the parameter $\alpha$ if we assume that the surveys observe the same source population, described by the same rate $r_0$. This assumption will in general be violated if different surveys have different frequency coverage or different observational strategies. Specifically, the observations of a deep and narrow survey will in general not be described by the same statistics as those of a shallow and wide survey, as explained by Connor et al. (2016d). Care is thus warranted when comparing detection numbers of qualitatively different surveys. Such an attempt will require more parameters or simply setting

$$P(n|r_0, \alpha) = 1 \tag{1.26}$$

for all surveys that are not expected to be described by $r_0$.

## 1.8   Data and results

We make use of 15 observed FRBs from seven surveys. For definiteness, we list all values used in our calculation in Tables 1.1 and 1.2. For the likelihood of the numbers of detected FRBs, we only make use of two dedicated pulsar surveys with well-defined characteristics, namely the High Time Resolution Universe Pulsar Survey (HTRU; Keith et al. 2010b) at the Parkes telescope and the Pulsar ALFA survey (PALFA; Cordes et al. 2006) at the Arecibo Observatory. We choose these two surveys because for most other discovered FRBs it is hard to estimate the surveying period $T$ that has been searched for FRBs, especially in the case of non-detections. The survey of Masui et al. (2015b) is similarly well-defined, but sensitive to different frequencies. We assume our parameter $r_0$ to describe the rate at frequencies around $1.4\,\mathrm{GHz}$ and do not want to make any assumption about the relation between this rate and the rate at $800\,\mathrm{MHz}$, which is the central frequency of Masui et al. (2015b).

Even for HTRU and PALFA, the parameters needed in Eq. (1.20) are defined somewhat ambiguously. To avoid building complicated models of the telescopes and surveys, we generally opt for simple choices that can be made consistently for both surveys. Specifically, this means that we do not include any estimate of the sky temperature due to the Milky Way in the values we assume for the system temperature $T_{\mathrm{sys}}$. For the gain $G$ we use the arithmetic mean of the gains corresponding to the beam centres of the multi-beam receivers. The bandwidth $B$ does not include frequencies deemed unusable by the surveying team and the angular size of the field of view $\Omega$ is intended to approximate the area within the half-maximum beam power. The resulting numerical values are listed in

Table 1.1: Parameters assumed for the FRB surveys.   See Sect. 1.7.2 for the meaning of the symbols.

| survey[1] | $s_{min}$ | $T_{sys}$/K | $G$/(K/Jy) | $n_p$ | $B$/MHz | $\Omega$/(deg$^2$) | $T$/h | $n$ |
|---|---|---|---|---|---|---|---|---|
| HTRU [1] | 10 | 23 | 0.64 | 2 | 340 | $13 \times 0.043$ | 3650 | 9 |
| PALFA [2] | 7 | 30 | 8.5 | 2 | 300 | $7 \times 0.0027$ | 886 | 1 |

[1] [1] Champion et al. 2015b; Thornton et al. 2013b; Keith et al. 2010b; [2] Spitler et al. 2014b; Cordes et al. 2006

Table 1.1. Other reasonable choices for these parameters will typically lead to deviations on the order of 10%. Note that the exact definition of each parameter does not impact the results as long as the same definition is used for all surveys that are being compared.

For the constraint on $\alpha$ coming from the likelihood for the observed signal-to-noise ratios, we can use all detected FRBs, as long as there is a well-defined signal-to-noise cutoff $s_{min}$. Since we are investigating the population of sources, we are not including repeated bursts from the same object (Spitler et al., 2016). We also exclude the single burst detections by Lorimer et al. (2007b) and Keane et al. (2011), since no definitive value of $s_{min}$ can be determined. We list the values of $s$ and $s_{min}$ that we use in Table 1.2.

After calculating the two-dimensional posterior for $\alpha$ and $r_0$, we derive the final constraint on $\alpha$ by marginalising over $r_0$ and vice versa. These posterior distributions are shown in Fig. 1.4.

## 1.9  Conclusions

The search for FRBs with multiple surveys that have disparate sensitivities, frequency coverage, and survey strategy (not to mention non-publication bias) has made it difficult even to estimate a daily sky rate. That combined with the relatively low number of total FRBs observed has meant that dealing with their statistics can be non-trivial. In the case of repetition, we remind the reader that several non-cataclysmic models for FRBs are expected to repeat. In the case of supergiant pulses from pulsars, SGR radio flares, or even Galactic flare stars, it is possible that this repetition would be non-stationary and might exhibit strong correlations in time. We have shown that if the repetition had some associated flicker noise and its power spectrum were $1/f^\gamma$, then one should expect the repetition rate to be higher immediately after the initial FRB detection. Therefore follow-up observations to archival discoveries that take place years or months after the first event would not provide strong upper limits. This would also mean that if no burst is found in a given beam after some integration time, then it is unlikely that one will

Table 1.2: Parameters of each individual FRB used in our calculation. The signal-to-noise ratios $s$ are taken from the FRBcat website[1] (Petroff et al., 2016).

| name | $s$ | $s_{min}$ | survey[2] |
|------|-----|-----------|-----------|
| FRB090625 | 30 | 10 | [1] |
| FRB110220 | 49 | 10 | [1] |
| FRB110626 | 11 | 10 | [1] |
| FRB110703 | 16 | 10 | [1] |
| FRB120127 | 11 | 10 | [1] |
| FRB121002 | 16 | 10 | [1] |
| FRB130626 | 21 | 10 | [1] |
| FRB130628 | 29 | 10 | [1] |
| FRB130729 | 14 | 10 | [1] |
| FRB121102 | 14 | 7 | [2] |
| FRB010125 | 17 | 7 | [3] |
| FRB131104 | 30 | 8 | [4] |
| FRB140514 | 16 | 10 | [5] |
| FRB150418 | 39 | 10 | [6] |
| FRB110523 | 42 | 8 | [7] |

[1] http://www.astronomy.swin.edu.au/pulsar/frbcat/

[2] [1] Champion et al. 2015b; Thornton et al. 2013b; Keith et al. 2010b; [2] Spitler et al. 2014b; Scholz et al. 2016; [3] Burke-Spolaor & Bannister 2014b; [4] Ravi et al. 2015; [5] Petroff et al. 2015b; [6] Keane et al. 2016b; [7] Masui et al. 2015b; Connor et al. 2016b
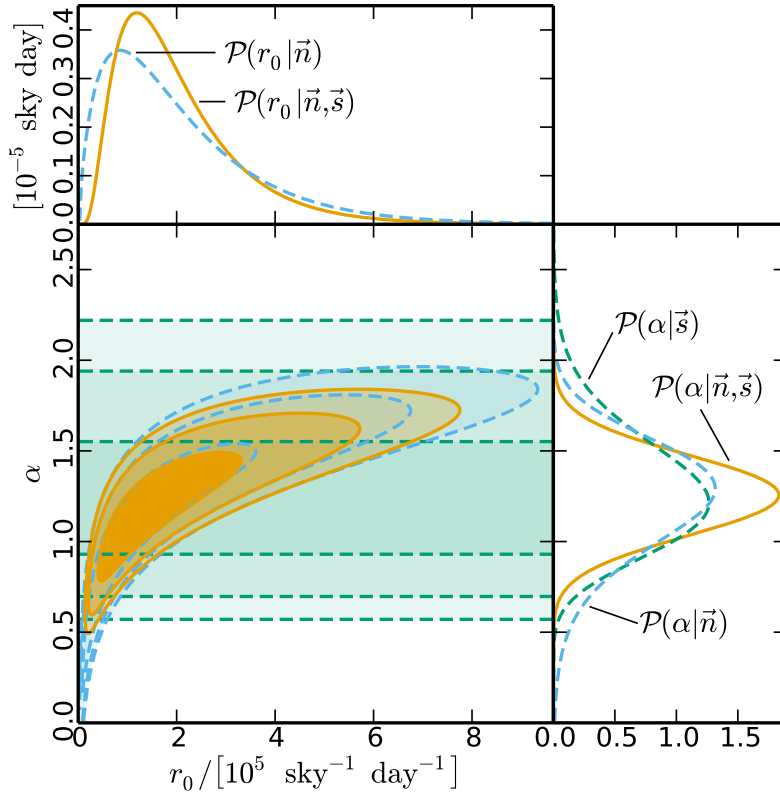
Figure 1.4: Posterior distribution for the parameter $\alpha$ describing the distribution of FRB flux densities and the FRB rate $r_0$. The bottom left panel shows the two-dimensional posterior for both parameters, the smaller panels show the marginalised posteriors for each parameter individually. We show separate curves and contours for the constraints coming from the signal-to-noise ratios $\vec{s}$ (green dashed), from the detection numbers $\vec{n}$ (blue dashed), and their combination (orange solid). The contour lines show the 68%, 95%, and 99% confidence regions.

occur in the following integration, and therefore a new pointing should be searched. In other words, shallow fast surveys would be favourable.

In Section 1.5 we offered a simple way of quantifying the latitudinal dependence of FRBs with a binomial distribution. This is akin to a biased coin flip, in which we ask "what is the probability of $M$ bursts being found in one region and $N$ bursts in its complement, given $\alpha$ times more time was spent in the former". Like Rane et al. (2015) we argue that the jury is still out on the severity of the latitudinal dependence. With current data the preference for FRBs to be discovered outside of the plane seems consistent with sky-temperature effects and increased scattering, or even pure chance. Whether or not more sophisticated explanations (e.g., Macquart & Johnston 2015) are required remains to be seen. We also provided a Bayesian framework for model comparison, which can be

used in the limit where large numbers of FRBs have been detected.

## 1.10 Conclusions

FRB 110523 is the only FRB to be observed below $1.4 \, \text{GHz}$. Its detection is encouraging because there are several upcoming surveys below a GHz whose impact on FRB science is hard to overestimate, so long as the transients are detectable at low frequencies. In the next several years CHIME, HIRAX, Tianlai, UTMOST, and ALERT could increase the number of detected FRBs by orders of magnitude, provide polarization information and repetition statistics, and localize them. In this paper we have provided the first detailed bounded constraints on the FRB rate below 1.4 GHz.

We have shown two ways of estimating the rate given the detection of FRB 110523, one based on a frequentist hypothesis test, and the other done in a Bayesian framework. These give the same maximum-likelihood value, but somewhat different 95% confidence intervals. We have then used the GBTIM estimate to forecast rates for CHIME and UTMOST, explicitly only comparing surveys with similar specifications. We find CHIME could detect between 2 and 40 per day, given by $\approx 7.5 \left( \frac{50 \, \text{K}}{T^{\text{sys}}} \right)^{1.5} \, \text{day}^{-1}$, making it the fastest upcoming survey. UTMOST, which observes in a band inside GBTIM's and whose sensitivity per steradian should eventually be comparable, could see between a couple per day and one every two weeks. We also found that CHIME Pathfinder's single formed beam, the nearby 26 m John A. Galt Telescope, and the 46 m ARO might see a couple FRBs each year, providing sub-arcsecond localisation through VLBI.

The difficulties of estimating an all-sky rate above a single fluence value was discussed. We showed how an on-sky rate not attached to a specific survey is not only hard to predict but also hard to interpret. For that reason we estimated a rate above the true threshold for GBTIM — an SNR of 8 — which gave us $2.7^{+12.4}_{-2.1} \times 10^4 \, \text{sky}^{-1} \, \text{day}^{-1}$. The fluences to which GBTIM was sensitive are those above the curve $0.17 \sqrt{(\tau/\text{ms})} \, \text{Jy} \, \text{ms}$ for pulse widths between 1-100 ms. To test the agreement between this rate and those found by other surveys, we scaled based only on thermal sensitivity. If we extrapolate from this daily rate to a survey with the sensitivity of HTRU, we find $6.4^{+29.5}_{-5.0} \times 10^3 \, \text{sky}^{-1} \, \text{day}^{-1}$, which is consistent with (Champion et al., 2015a).

We also investigated the flux distribution index, $\gamma$, and found that steep distributions with $\gamma > 2.2$ are ruled out.

# Chapter 2

# Conclusions and Outlook

# Bibliography

Bandura, K. e. a. 2014, in Society of Photo-Optical Instrumentation Engineers (SPIE) Conference Series, Vol. 9145, Society of Photo-Optical Instrumentation Engineers (SPIE) Conference Series, 22

Burke, B. F., & Graham-Smith, F. 2014, An Introduction to Radio Astronomy

Burke-Spolaor, S., & Bannister, K. W. 2014a, ApJ, 792, 19

—. 2014b, ApJ, 792, 19

Caleb, M., Flynn, C., Bailes, M., et al. 2016a, MNRAS, 458, 708

—. 2016b, ArXiv e-prints 1601.02444, arXiv:1601.02444

Champion, D. J., Petroff, E., Kramer, M., et al. 2015a, ArXiv e-prints 1511.07746, arXiv:1511.07746

—. 2015b, ArXiv e-prints, arXiv:1511.07746

Chang, T.-C., Pen, U.-L., Bandura, K., & Peterson, J. B. 2010, Nature, 466, 463

Connor, L., Lin, H.-H., Masui, K., et al. 2016a, MNRAS, 460, 1054

—. 2016b, ArXiv e-prints, arXiv:1602.07292

Connor, L., Pen, U.-L., & Oppermann, N. 2016c, MNRAS, 458, L89

—. 2016d, MNRAS, 458, L89

—. 2016e, MNRAS, arXiv:1601.04051

Connor, L., Sievers, J., & Pen, U.-L. 2015, ArXiv e-prints, arXiv:1505.05535

—. 2016f, MNRAS, 458, L19

Cordes, J. M., Freire, P. C. C., Lorimer, D. R., et al. 2006, ApJ, 637, 446

Keane, E. F., Kramer, M., Lyne, A. G., Stappers, B. W., & McLaughlin, M. A. 2011, MNRAS, 415, 3065

Keane, E. F., & Petroff, E. 2015, MNRAS, 447, 2852

Keane, E. F., Stappers, B. W., Kramer, M., & Lyne, A. G. 2012, MNRAS, 425, L71

Keane, E. F., Johnston, S., Bhandari, S., et al. 2016a, Nature, 530, 453

—. 2016b, Nature, 530, 453

Keith, M. J., Jameson, A., van Straten, W., et al. 2010a, MNRAS, 409, 619

—. 2010b, MNRAS, 409, 619

Kulkarni, S. R., Ofek, E. O., & Neill, J. D. 2015, ArXiv e-prints 1511.09137, arXiv:1511.09137

Law, C. J., Bower, G. C., Burke-Spolaor, S., et al. 2015, ApJ, 807, 16

Lorimer, D. R., Bailes, M., McLaughlin, M. A., Narkevic, D. J., & Crawford, F. 2007a, Science, 318, 777

—. 2007b, Science, 318, 777

Macquart, J.-P., & Johnston, S. 2015, MNRAS, 451, 3278

Maoz, D., Loeb, A., Shvartzvald, Y., et al. 2015, ArXiv e-prints 1507.01002, arXiv:1507.01002

Masui, K., Lin, H.-H., Sievers, J., et al. 2015a, Nature, 528, 523

—. 2015b, Nature, 528, 523

Milotti, E. 2002, ArXiv Physics e-prints, physics/0204033

Mottez, F., & Zarka, P. 2014, A&A, 569, A86

Ogasaka, Y., Murakami, T., Nishimura, J., Yoshida, A., & Fenimore, E. E. 1991, ApJ, 383, L61

Oppermann, N., Connor, L., & Pen, U.-L. 2016, ArXiv e-prints, arXiv:1604.03909

Pen, U.-L., & Connor, L. 2015, ApJ, 807, 179

Petroff, E., van Straten, W., Johnston, S., et al. 2014, ApJ, 789, L26

Petroff, E., Bailes, M., Barr, E. D., et al. 2015a, MNRAS, 447, 246

—. 2015b, MNRAS, 447, 246

Petroff, E., Johnston, S., Keane, E. F., et al. 2015c, MNRAS, 454, 457

Petroff, E., Barr, E. D., Jameson, A., et al. 2016, ArXiv e-prints, arXiv:1601.03547

Popov, S. B., & Postnov, K. A. 2007, ArXiv e-prints, arXiv:0710.2006

Press, W. H. 1978, Comments on Astrophysics, 7, 103

Rane, A., Lorimer, D. R., Bates, S. D., et al. 2015, ArXiv e-prints 1505.00834, arXiv:1505.00834

—. 2016, MNRAS, 455, 2207

Ravi, V., Shannon, R. M., & Jameson, A. 2015, ApJ, 799, L5

Schmidt, M. 1968a, ApJ, 151, 393

—. 1968b, ApJ, 151, 393

Scholz, P., Spitler, L. G., Hessels, J. W. T., et al. 2016, ArXiv e-prints, arXiv:1603.08880

Shaw, J. R., Sigurdson, K., Sitwell, M., Stebbins, A., & Pen, U.-L. 2015, Phys. Rev. D, 91, 083514

Spitler, L. G., Cordes, J. M., Hessels, J. W. T., et al. 2014a, ApJ, 790, 101

—. 2014b, ApJ, 790, 101

Spitler, L. G., Scholz, P., Hessels, J. W. T., et al. 2016, Nature, 531, 202

Switzer, E. R., Masui, K. W., Bandura, K., et al. 2013, MNRAS, 434, L46

Thornton, D., Stappers, B., Bailes, M., et al. 2013a, Science, 341, 53

—. 2013b, Science, 341, 53

van Leeuwen, J. 2014, in The Third Hot-wiring the Transient Universe Workshop, ed. P. R. Wozniak, M. J. Graham, A. A. Mahabal, & R. Seaman, 79–79

Vedantham, H. K., Ravi, V., Hallinan, G., & Shannon, R. 2016, ArXiv e-prints, arXiv:1606.06795

Verheijen, M. A. W., Oosterloo, T. A., van Cappellen, W. A., et al. 2008, in American Institute of Physics Conference Series, Vol. 1035, The Evolution of Galaxies Through the Neutral Hydrogen Window, ed. R. Minchin & E. Momjian, 265–271

Voss, R. F., & Clarke, J. 1975, Nature, 258, 317

Williams, P. K. G., & Berger, E. 2016, ApJ, 821, L22